CASE FILE
COPY

NATIONAL ADVISORY COMMITTEE FOR AERONAUTICS

REPORT No. 684

STATIC THRUST AND POWER CHARACTERISTICS OF SIX FULL-SCALE PROPELLERS

By EDWIN P. HARTMAN and DAVID BIERMANN



1940

For sale by the Superintendent of Documents, Washington, D. C. - - - - - - - - - - - - - - - Price 10 cents

AERONAUTIC SYMBOLS

1. FUNDAMENTAL AND DERIVED UNITS

	Symbol	Metric		English	
		Unit	Abbreviation	Unit	Abbreviation
Length	l	meter	m	foot (or mile)	ft. (or mi.)
Time	t	second	s	second (or hour)	sec. (or hr.)
Force	F	weight of 1 kilogram	kg	weight of 1 pound	lb.
Power	P	horsepower (metric)		horsepower	hp.
Speed	V	kilometers per hour	k.p.h.	miles per hour	m.p.h.
		meters per second	m.p.s.	feet per second	f.p.s.

2. GENERAL SYMBOLS

W, Weight$=mg$

g, Standard acceleration of gravity$=9.80665$ m/s^2 or 32.1740 ft./sec.^{2}

m, Mass$=\frac{W}{g}$

I, Moment of inertia$=mk^2$. (Indicate axis of radius of gyration k by proper subscript.)

μ, Coefficient of viscosity

ν, Kinematic viscosity

ρ, Density (mass per unit volume)

Standard density of dry air, 0.12497 kg-m^{-4}-s^2 at 15° C. and 760 mm; or 0.002378 lb.-ft.$^{-4}$ sec.^{2}

Specific weight of "standard" air, 1.2255 kg/m^3 or 0.07651 lb./cu. ft.

3. AERODYNAMIC SYMBOLS

S, Area

S_w, Area of wing

G, Gap

b, Span

c, Chord

$\frac{b^2}{S}$, Aspect ratio

V, True air speed

q, Dynamic pressure$=\frac{1}{2}\rho V^2$

L, Lift, absolute coefficient $C_L=\frac{L}{qS}$

D, Drag, absolute coefficient $C_D=\frac{D}{qS}$

D_0, Profile drag, absolute coefficient $C_{D_0}=\frac{D_0}{qS}$

D_i, Induced drag, absolute coefficient $C_{D_i}=\frac{D_i}{qS}$

D_p, Parasite drag, absolute coefficient $C_{D_p}=\frac{D_p}{qS}$

C, Cross-wind force, absolute coefficient $C_C=\frac{C}{qS}$

R, Resultant force

i_w, Angle of setting of wings (relative to thrust line)

i_t, Angle of stabilizer setting (relative to thrust line)

Q, Resultant moment

Ω, Resultant angular velocity

$\rho\frac{Vl}{\mu}$, Reynolds Number, where l is a linear dimension (e.g., for a model airfoil 3 in. chord, 100 m.p.h. normal pressure at 15° C., the corresponding number is 234,000; or for a model of 10 cm chord, 40 m.p.s., the corresponding number is 274,000)

C_p, Center-of-pressure coefficient (ratio of distance of c.p. from leading edge to chord length)

α, Angle of attack

ϵ, Angle of downwash

α_0, Angle of attack, infinite aspect ratio

α_i, Angle of attack, induced

α_a, Angle of attack, absolute (measured from zero-lift position)

γ, Flight-path angle

REPORT No. 684

STATIC THRUST AND POWER CHARACTERISTICS OF SIX FULL-SCALE PROPELLERS

By EDWIN P. HARTMAN and DAVID BIERMANN
Langley Memorial Aeronautical Laboratory

222645—40——1

NATIONAL ADVISORY COMMITTEE FOR AERONAUTICS

HEADQUARTERS, NAVY BUILDING, WASHINGTON, D. C.

LABORATORIES, LANGLEY FIELD, VA.

Created by act of Congress approved March 3, 1915, for the supervision and direction of the scientific study of the problems of flight (U. S. Code, Title 50, Sec. 151). Its membership was increased to 15 by act approved March 2, 1929. The members are appointed by the President, and serve as such without compensation.

VANNEVAR BUSH, Sc. D., *Chairman*,
Washington, D. C.

GEORGE J. MEAD, Sc. D., *Vice Chairman*,
West Hartford, Conn.

CHARLES G. ABBOT, Sc. D.,
Secretary, Smithsonian Institution.

HENRY H. ARNOLD, Major General, United States Army,
Chief of Air Corps, War Department.

GEORGE H. BRETT, Brigadier General, United States Army,
Chief Matériel Division, Air Corps, Wright Field, Dayton, Ohio.

LYMAN J. BRIGGS, Ph. D.,
Director, National Bureau of Standards.

ROBERT E. DOHERTY, M. S.,
Pittsburgh, Pa.

CLINTON M. HESTER, A. B., LL. B.,
Administrator, Civil Aeronautics Authority.

ROBERT H. HINCKLEY, A. B.,
Chairman, Civil Aeronautics Authority.

JEROME C. HUNSAKER, Sc. D.,
Cambridge, Mass.

SYDNEY M. KRAUS, Captain, United States Navy,
Bureau of Aeronautics, Navy Department.

FRANCIS W. REICHELDERFER, Sc. D.,
Chief, United States Weather Bureau.

JOHN H. TOWERS, Rear Admiral, United States Navy,
Chief, Bureau of Aeronautics, Navy Department.

EDWARD WARNER, Sc. D.,
Washington, D. C.

ORVILLE WRIGHT, Sc. D.,
Dayton, Ohio.

GEORGE W. LEWIS, *Director of Aeronautical Research* S. PAUL JOHNSTON, *Coordinator of Research*

JOHN F. VICTORY, *Secretary*

HENRY J. E. REID, *Engineer in Charge, Langley Memorial Aeronautical Laboratory, Langley Field, Va.*

JOHN J. IDE, *Technical Assistant in Europe, Paris, France*

TECHNICAL COMMITTEES

AERODYNAMICS
POWER PLANTS FOR AIRCRAFT
AIRCRAFT MATERIALS

AIRCRAFT STRUCTURES
AIRCRAFT ACCIDENTS
INVENTIONS AND DESIGNS

Coordination of Research Needs of Military and Civil Aviation

Preparation of Research Programs

Allocation of Problems

Prevention of Duplication

Consideration of Inventions

LANGLEY MEMORIAL AERONAUTICAL LABORATORY

LANGLEY FIELD, VA.

Unified conduct, for all agencies, of scientific research on the fundamental problems of flight.

OFFICE OF AERONAUTICAL INTELLIGENCE

WASHINGTON, D. C.

Collection, classification, compilation, and dissemination of scientific and technical information on aeronautics.

4-1-40

REPORT No. 684

STATIC THRUST AND POWER CHARACTERISTICS OF SIX FULL-SCALE PROPELLERS

By Edwin P. Hartman and David Biermann

SUMMARY

Static thrust and power measurements were made of six full-scale propellers. The propellers were mounted in front of a liquid-cooled-engine nacelle and were tested at 15 different blade angles in the range from −7½° to 35° at 0.75R. The test rig was located outdoors and the tests were made under conditions of approximately zero wind velocity.

Airfoil characteristics computed from the static-test data, by the single-point method developed by Lock, were considerably different from the airfoil characteristics computed from wind-tunnel-test data for the same propeller and nacelle.

The tests showed a marked variation of static thrust and power coefficients with tip speed for the range of blade angles from about 7½° to 17½°. A propeller with R. A. F. 6 airfoil sections showed the greatest effect of compressibility and a propeller with N. A. C. A. 2400–34 series sections showed the least effect. A propeller with a wide blade showed much less effect of compressibility than a similar propeller with a blade of normal width.

INTRODUCTION

The static thrust and torque of a full-scale propeller (the thrust and the torque at $V/nD=0$) are difficult to obtain in a wind tunnel because the propeller itself creates a considerable air velocity through the tunnel. Conditions of zero V/nD are, therefore, never reached in normal wind-tunnel propeller tests.

Static thrust and torque measurements of propellers, if properly interpreted, may give considerable information regarding the flight performance of the propellers. Such measurements are especially useful for studying the effect of compressibility and also for comparing propellers with different airfoil sections, plan forms, and solidities.

Static thrust is often used in take-off calculations and is a basic parameter in Diehl's take-off formulas (reference 1). To facilitate the use of his formulas, Diehl has collected a mass of static-thrust data, which are mostly extrapolated data from wind-tunnel tests, for a fairly large group of propellers (reference 2). The material given in reference 2, although it fulfills its purpose admirably, lacks the completeness, the correlation, and the precision necessary for a differential study of propeller characteristics. Other useful, but somewhat incomplete, static-thrust data are given in reference 3.

Comparisons of the performance characteristics of propellers are clarified through the use of the single-point method developed by Lock (reference 4), by means of which test data for a propeller obtained in a wind tunnel can easily be converted to airfoil coefficients (C_L and C_D) representing the propeller. Through a modification of Lock's method, Driggs (reference 5) has developed an alternative method having possible advantages over Lock's method. Both methods imply that the airfoil characteristics representing the propeller may be obtained from either wind-tunnel or static-test data, the same coefficients being obtained in either case. The theory indicates that static thrust and torque measurements of a propeller, obtained on a simple outdoor test rig, can be converted into airfoil coefficients and then reconverted into propeller data representing all conditions of V/nD, blade angle, and solidity. A few simple static-thrust tests would then conceivably be a substitute for a long series of expensive wind-tunnel tests.

It is the purpose of this report to present static-thrust and static-power data, for a group of propellers having modern plan forms, to be used:

(1) For practical purposes such as estimating take-off distances.

(2) To show the effects of variations in tip speed, airfoil section, and solidity on the static characteristics of propellers and to point out the implication of these static effects in connection with the flight performance of the propellers.

(3) To check the method of Lock and Driggs and to determine the quality of the substitution of static tests for wind-tunnel tests.

This report is the ninth of a series presenting the results of an extensive research program of full-scale propellers that has been in progress at the N. A. C. A. during the past 2 years.

APPARATUS AND METHODS

Test rig.—The test rig was located outdoors well clear of any buildings or objects that might have an appreciable influence on the air flow through the propeller. A photograph of the test set-up is shown in figure 1. A simplified sketch showing how the thrust was measured is given in figure 2. The rectangular frame upon which the engine is mounted is supported at its forward corners on ball bearings and at the rear

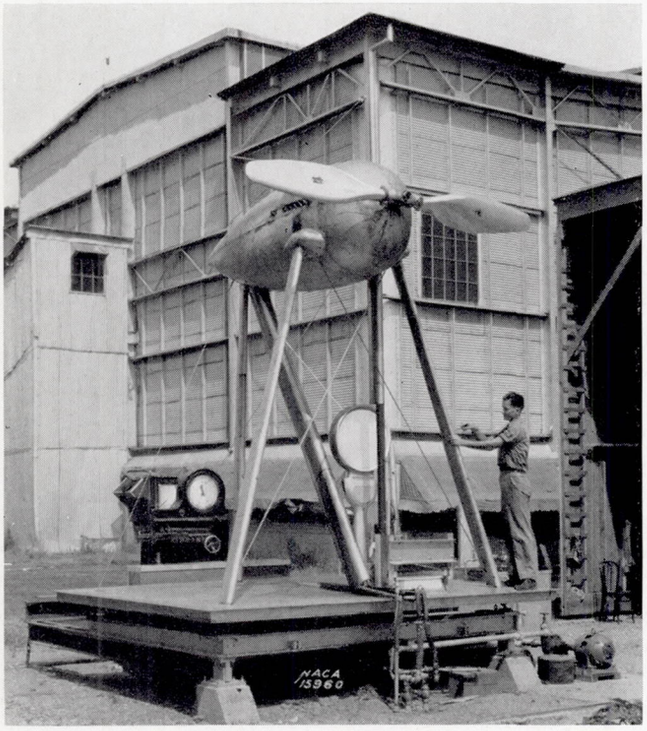


FIGURE 1.—Propeller 37–3647 mounted on test rig.

on knife edges bearing on the thrust-scale platform. The thrust of the propeller tends to rock the frame forward about the ball-bearing pivots and relieves the load on the thrust scale. The thrust is then equal to the change in thrust-scale reading times the ratio of the moment arms a/b. The drag, caused by the slipstream, of the body, the struts, and the wires registered on the scale as a negative component of the thrust.

Engine, nacelle, and dynamometer.—The engine, the nacelle, the struts, and the supporting frame are the same as used for the wind-tunnel tests reported in reference 6. The propellers were driven by a 600-horsepower Curtiss Conqueror engine (GIV-1570) enclosed in a liquid-cooled-engine nacelle of oval cross section. The nacelle was 126 inches in length, 38 inches in width, and 43 inches in height. The engine was mounted in a cradle free to rotate about an axis, at one side of the engine, parallel to the propeller axis. The other side of the cradle rested on a column that transmitted the torque forces to the platform of a scale, as shown in figure 1.

Propellers.—The blade-form curves for the six propellers tested are given in figure 3. Other basic characteristics of the propellers are given in the following table.

Propeller (Bureau of Aeronautics, Navy Department, drawing number)	Number of blades	Diameter (ft)	Blade airfoil section
5868–9	2	10	Clark Y.
5868–9	3	10	Do.
5868–R6	2	10	R. A. F. 6.
5868–R6	3	10	Do.
6623–B	2	10	N. A. C. A. 4400 series inner half. N. A. C. A. 2400–34 series outer half.
37–3647[a]	2	10	R. A. F. 6.

[a] Army Air Corps drawing number.

The propellers, except 37–3647, have plan forms representing modern design and have identical ratios of blade width and thickness. Propeller 37–3647 is the same as propeller 5868–R6 in every respect except that its blade-width ratio is 50 percent greater. Propeller 6623–B was designed to minimize the bad effects of compressibility, the N. A. C. A. 2400–34 series airfoil section used for the outer half being less affected

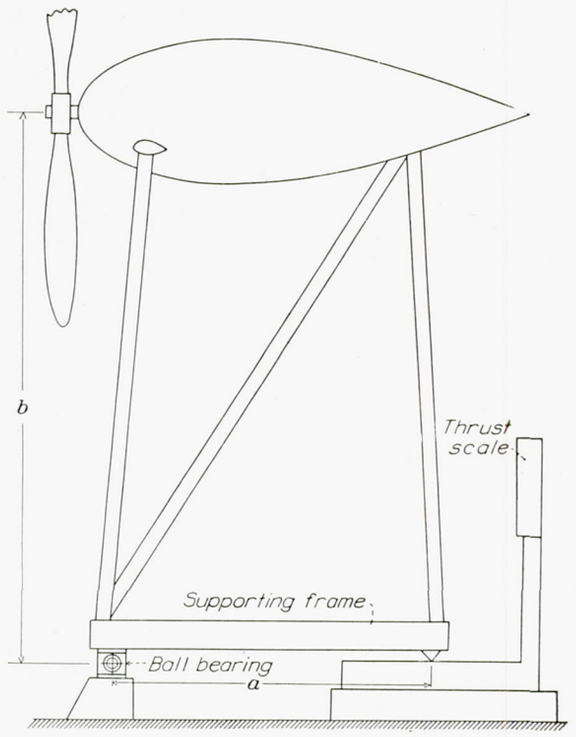


FIGURE 2.—Diagrammatic sketch showing method of measuring static thrust.

by compressibility than the usual propeller sections. The airfoil sections representing the $0.70R$ station for the propellers tested are shown in figure 4. The N. A. C. A. 4400 series sections of propeller 6623–B extended only to the $0.50R$ station; but for purposes of comparison the 4400 series section, as shown in figure 4, has a chord and a thickness representing the $0.70R$ station.

Tests.—The propellers were tested through a blade-angle range from $-7\frac{1}{2}°$ to 35°. Intervals of $2\frac{1}{2}°$ were

taken from $-7\frac{1}{2}°$ to 20° and intervals of 5° from 20° to 35°. Readings were taken at intervals of approxi-

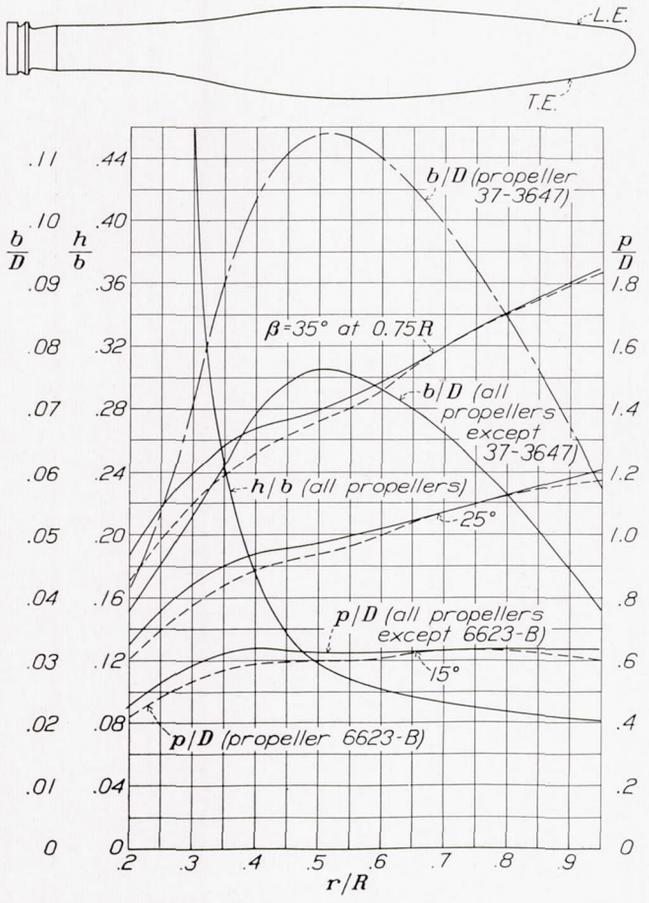


FIGURE 3.—Blade-form curves for propellers 5868–9, 5868–R6, 6623–B, and 37–3647 D, diameter; R, radius to the tip; r, station radius; b, section chord; h, section thickness; p, geometric pitch; β, blade angle.

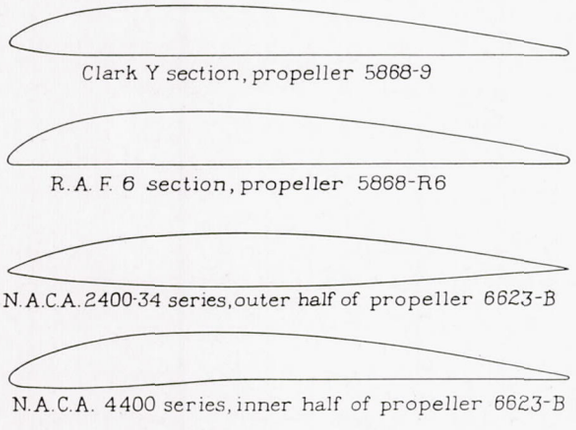


FIGURE 4.—Propeller blade sections; representative of the $0.70R$ station.

mately 200 rpm through a range of propeller speeds from 600 to 1,800 rpm for the lower blade angles and to full-throttle propeller speed for the higher blade angles.

Tests were made only on days when the wind velocity was zero or close to zero. A calibrated anemometer was used to measure the wind velocity.

RESULTS AND DISCUSSION

COEFFICIENTS AND SYMBOLS

The results are expressed in terms of the usual propeller coefficients defined as follows:

$C_T=\frac{T_e}{\rho n^2 D^4}$ thrust coefficient.

$C_P=\frac{P}{\rho n^3 D^5}$ power coefficient.

where

$T_e=T-\Delta D$ effective thrust, pounds.
T tension in propeller shaft, pounds.
ΔD change in drag of body due to slipstream, pounds.
ρ mass density of air, slugs per cubic foot.
n propeller speed, revolutions per second.
D propeller diameter, feet.
P engine power, foot-pounds per second.

Other coefficients and symbols used in the report are defined as follows:

$C_L=L/qS$ lift coefficient.
$C_D=D/qS$ drag coefficient.
$C_Q=Q/\rho n^2 D^5=C_P/2\pi$ torque coefficient.
L lift, pounds.
D drag, pounds.
q dynamic pressure, pounds per square foot.
S area, square feet.
Q torque, pound-feet.
M ratio of tip speed to speed of sound.
$x=r/R$
r station radius.
R radius to the tip.
$C_{D_0}=C_D-C_{D_i}$ effective profile-drag coefficient.
C_{D_i} induced-drag coefficient.
α_∞ angle of attack with respect to relative wind where the relative wind is the vector sum of the rotational, the forward, and the inflow velocities.

BASIC DATA

The basic data obtained in the tests are presented in figures 5 to 16 where, for each propeller, curves of C_T and C_P are plotted against M. Each of the curves in these figures is the average of several curves obtained from repeated tests at the same blade angle. Small corrections for wind were made when necessary.

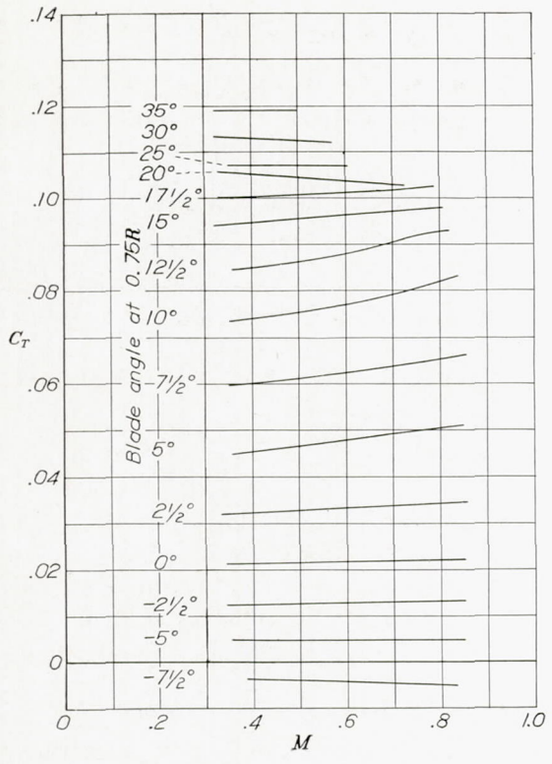


FIGURE 5.—Variation of static-thrust coefficient with tip-speed ratio and blade angle. Propeller 5868–9, 2 blades.

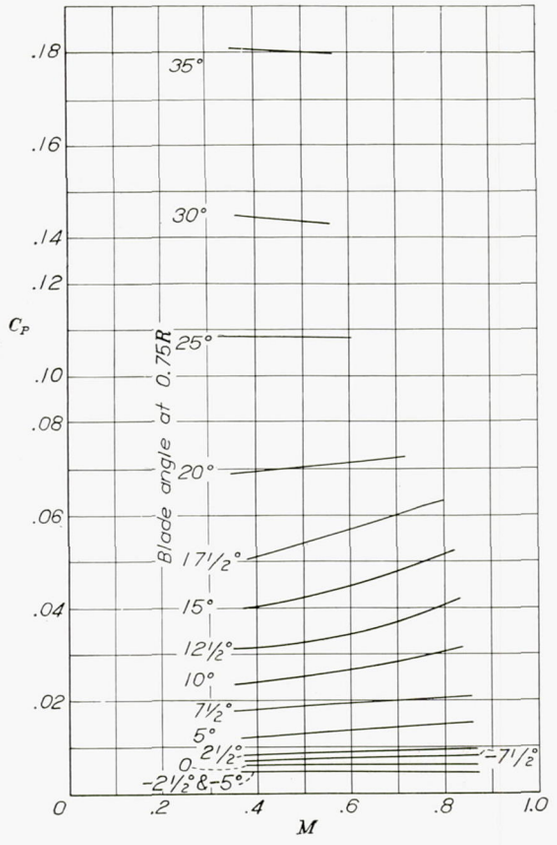


FIGURE 6.—Variation of static-power coefficient with tip-speed ratio and blade angle. Propeller 5868–9, 2 blades.

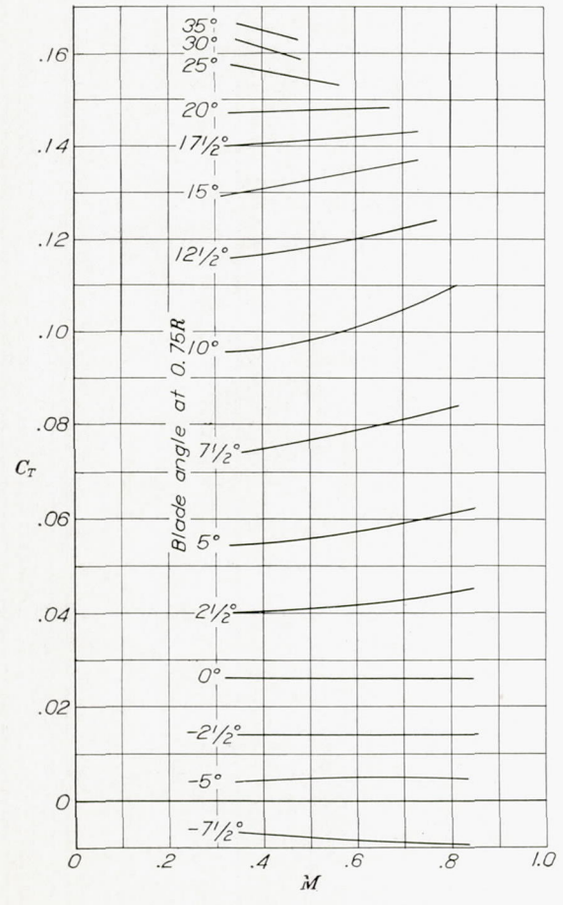


FIGURE 7.—Variation of static-thrust coefficient with tip-speed ratio and blade angle. Propeller 5868–9, 3 blades.

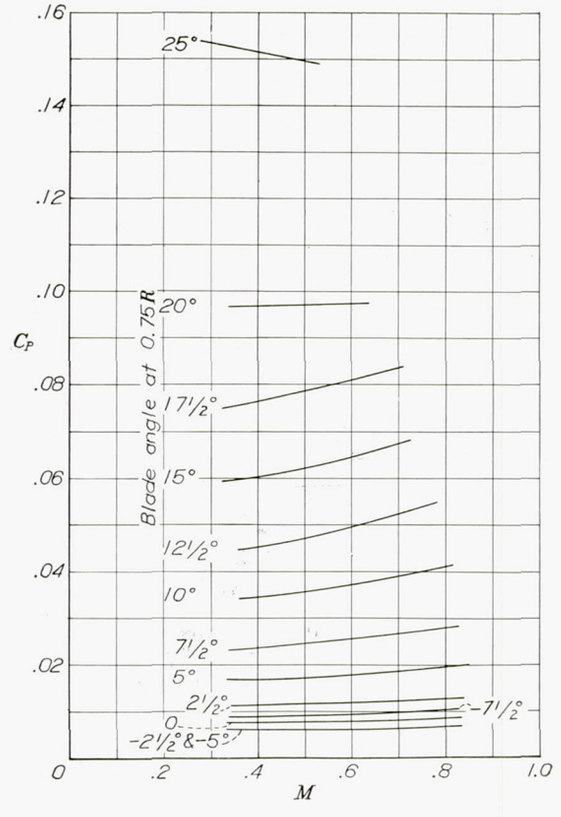


FIGURE 8.—Variation of static-power coefficient with tip-speed ratio and blade angle. Propeller 5868–9, 3 blades.

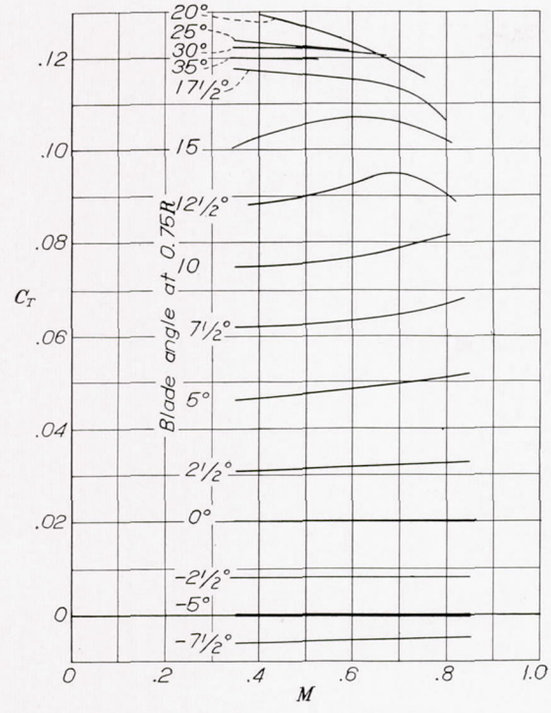


FIGURE 9.—Variation of static-thrust coefficient with tip-speed ratio and blade angle. Propeller 5868–R6, 2 blades.

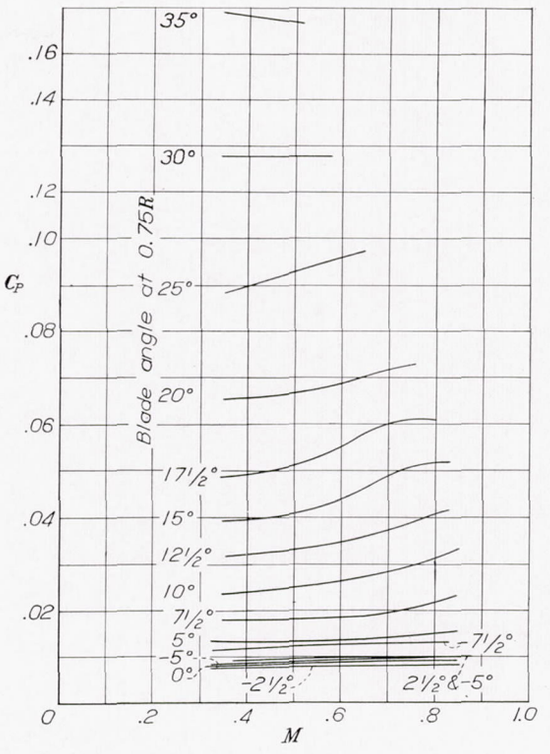


FIGURE 10.—Variation of static-power coefficient with tip-speed ratio and blade angle. Propeller 5868–R6, 2 blades.

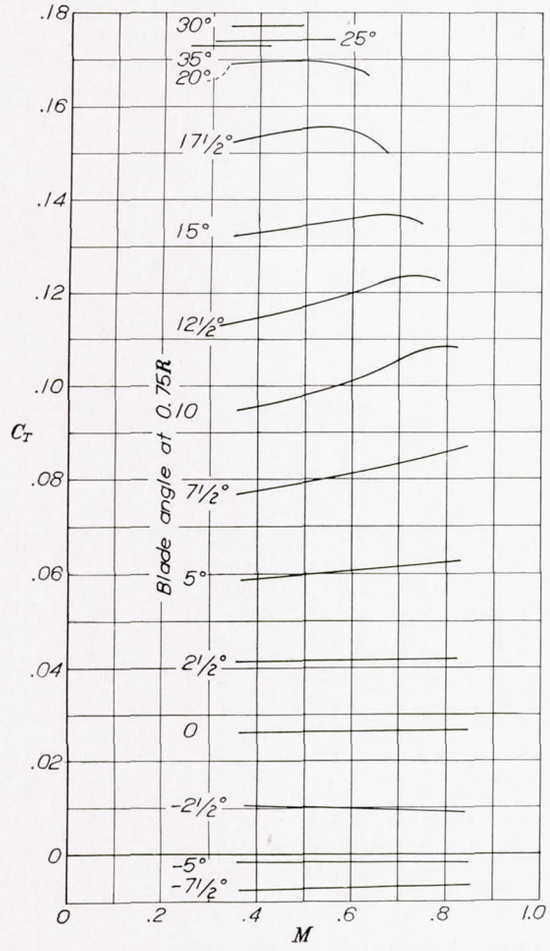


FIGURE 11.—Variation of static-thrust coefficient with tip-speed ratio and blade angle. Propeller 5868–R6, 3 blades.

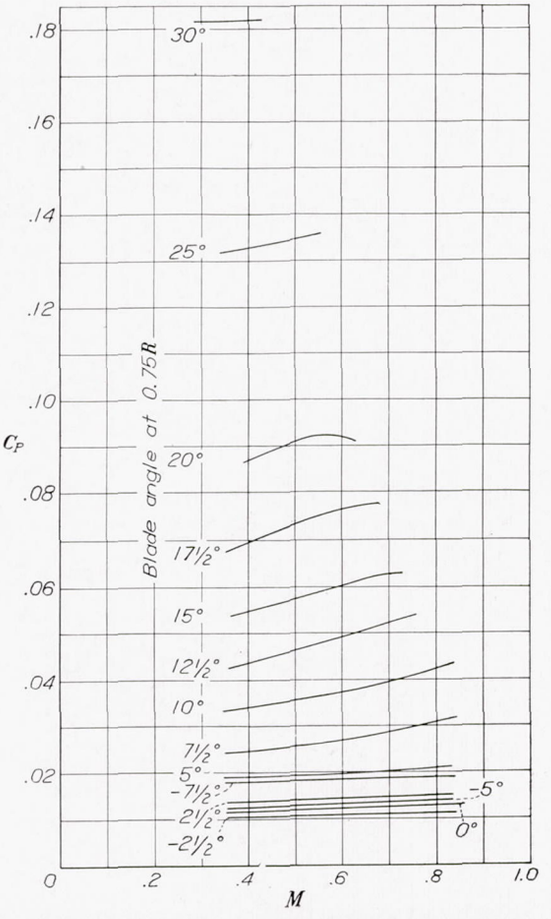


FIGURE 12.—Variation of static-power coefficient with tip-speed ratio and blade angle. Propeller 5868–R6, 3 blades.

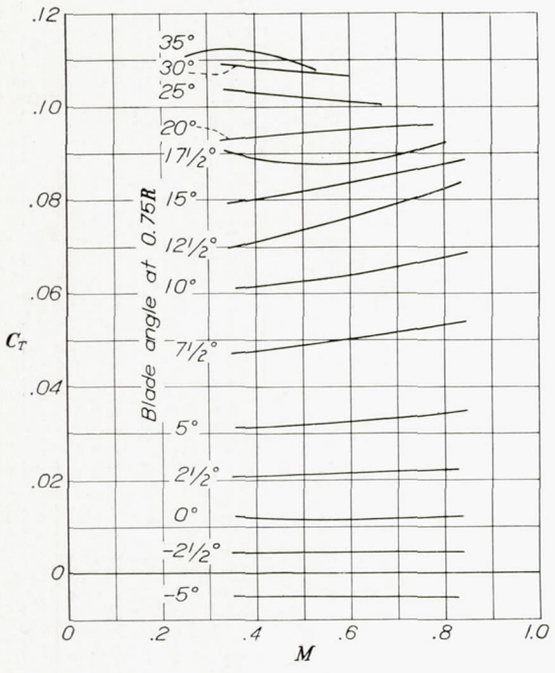


FIGURE 13.—Variation of static-thrust coefficient with tip-speed ratio and blade angle. Propeller 6623–B, 2 blades.

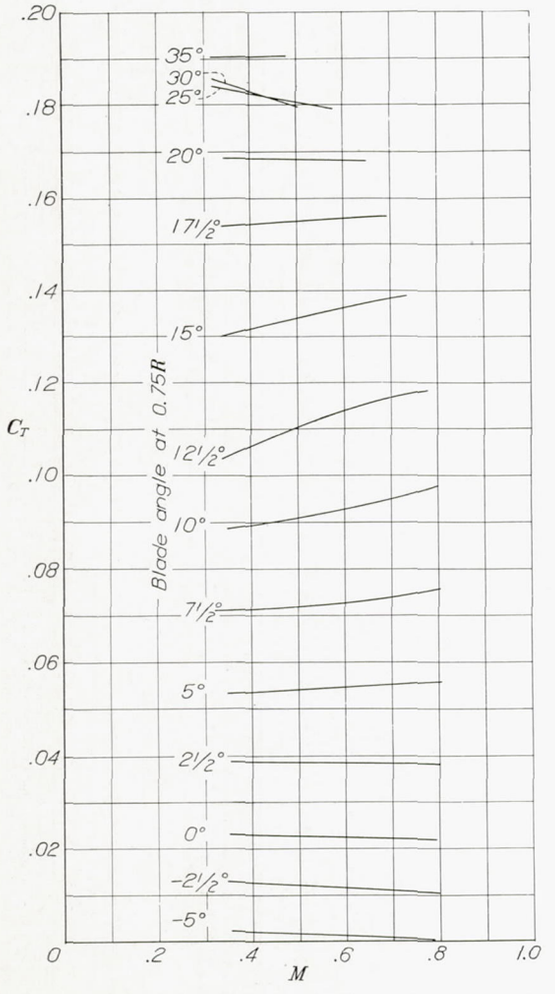


FIGURE 15.—Variation of static-thrust coefficient with tip-speed ratio and blade angle. Propeller 37–3647, 2 blades.

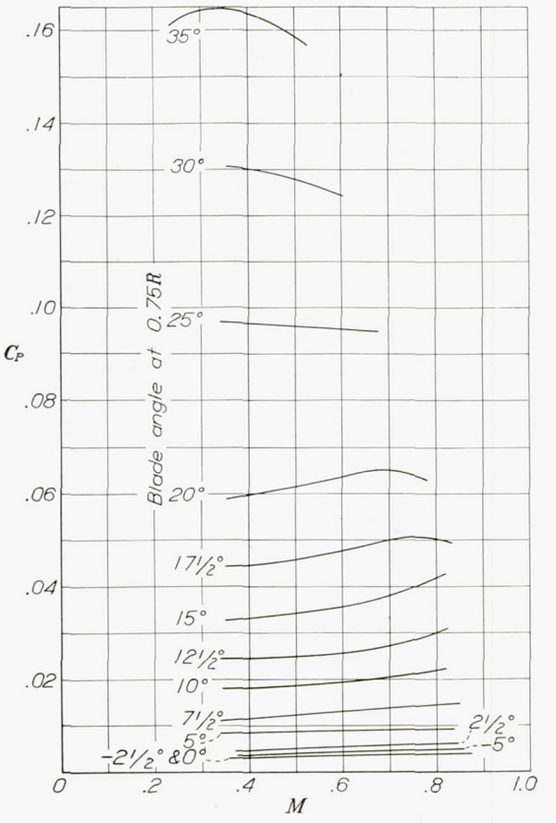


FIGURE 14.—Variation of static-power coefficient with tip-speed ratio and blade angle Propeller 6623–B, 2 blades.

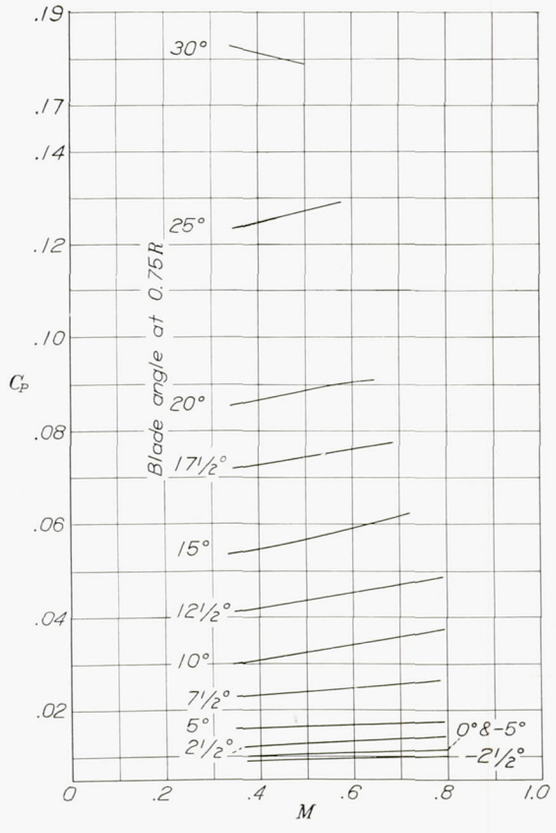


FIGURE 16.—Variation of static-power coefficient with tip-speed ratio and blade angle. Propeller 37–3647, 2 blades.

Effect of tip speed.—The curves in figures 5 to 16 show the variation of static-thrust and static-power coefficients with tip speed. The effect of compressibility is most noticeable in the range of blade angles from 5° to 17½°. Above the stall (about 17½°), there is no consistent effect that can be ascribed to compressibility in the range of tip speeds tested.

Previous work, both theoretical and experimental, indicates that the curves below the stall would be expected to rise gradually with increasing tip speed until the speed of sound is exceeded in the local flow around the blade tips. At this point, a shock wave would form and the thrust coefficient would begin to decrease, the decrease in thrust becoming greater as the tip speed increased and as more of the propeller blade became involved in local supersonic air flows. The present tests seem to confirm the theory, although only propeller 5868–R6 appears, from the shape of the thrust-coefficient curves, to have reached the compressibility stall.

A clearer idea of the way in which compressibility affects propeller performance is obtained by converting the propeller coefficients into airfoil coefficients by a method to be discussed later. This conversion has been made for the 2-blade propeller 5868–R6 set at 15° and the coefficients C_L, C_D, C_{D_i}, and C_{D_0} have been plotted against the tip-speed ratio M in figure 17. The compressibility stall is determined as the point where the profile-drag coefficient begins its sharp rise. The peak of the lift-coefficient curve is usually slightly beyond that point. The decrease in induced-drag coefficient beyond the compressibility stall, due to loss of lift, only slightly offsets the sudden increase in profile drag. It should be pointed out that the tip speed (value of M) at which the compressibility stall occurs will depend largely on the propeller airfoil section and the lift coefficient. The following relation indicating the incipience of the compressibility stall represents the conditions with reasonable accuracy.

$$M_{stall}=M_0-k\,C_L$$

In this formula, which applies only below the normal stall, M_0 and k are constants determined largely by the airfoil characteristics of the propeller but also varying with the solidity and the plan form.

Static-thrust figure of merit.—The efficiency of a propeller in producing static thrust is best indicated by the magnitude of the ratio of thrust produced to the power supplied, i. e., T_e/P. Unfortunately, this figure of merit, which has dimensions, cannot be represented by the ratio of the dimensionless coefficients C_T/C_P because

$$\frac{C_T}{C_P}=\frac{T_e\rho n^3D^5}{P\rho n^2D^4}=\frac{T_e}{P}nD$$

or

$$\frac{T_e}{P}=\frac{C_T/C_P}{nD}$$

This relation indicates that, for any given value of the ratio C_T/C_P, the thrust per unit of power decreases as the tip speed increases. The ratio C_T/C_P may, however, be used as a figure of merit for comparing propellers at constant tip speed.

Comparisons of tip-speed effects.—Figures 18 and 19 show the ratio $(C_T/C_P)/(C_T/C_P)_{M=0.5}$ plotted against the tip-speed ratio M for the six propellers tested. Measuring from $M=0.5$, the curves give directly the percentage loss in C_T/C_P for other values of M. The

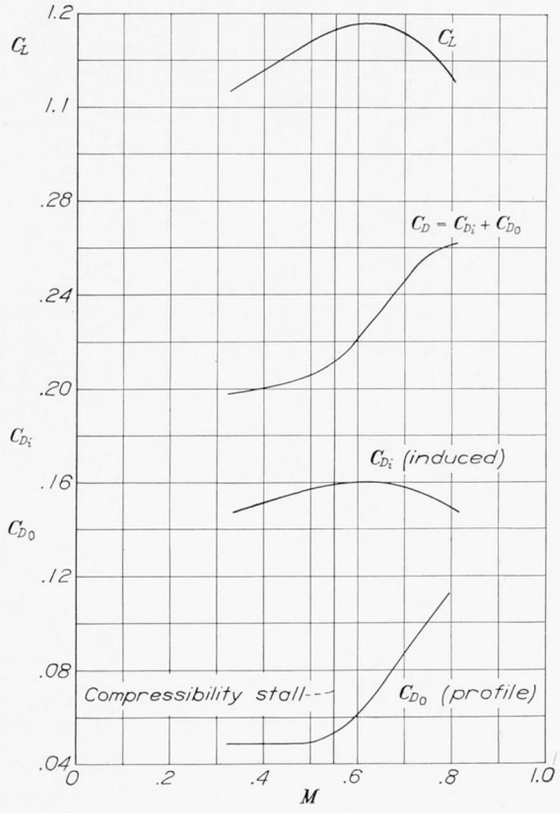


FIGURE 17.—Effect of compressibility on airfoil coefficients obtained from the static-test propeller coefficients for 2-blade propeller 5868–R6 set 15° at 0.75R.

curves show that, although the C_T curves increase with M, as shown in figures 5, 7, 9, 11, and 13, the ratio C_T/C_P decreases with increasing values of M. The curves also show that the propellers with the R. A. F. 6 section are, in general, most affected by compressibility and that propeller 6623–B with the N. A. C. A. 2400–34 series section in the outer half is least affected.

Another point of interest in figures 18 and 19 is that the 3-blade propellers generally are less affected by compressibility than the 2-blade propellers with the exception of the 2-blade propeller 37–3647 which, although it has an R. A. F. 6 section, showed little effect of compressibility throughout the range of tip speeds tested. This phenomenon, which is confirmed by the wind-tunnel tests reported in reference 7, seems to indicate some relationship between compressibility and plan form, or blade-width ratio.

222645—40——2

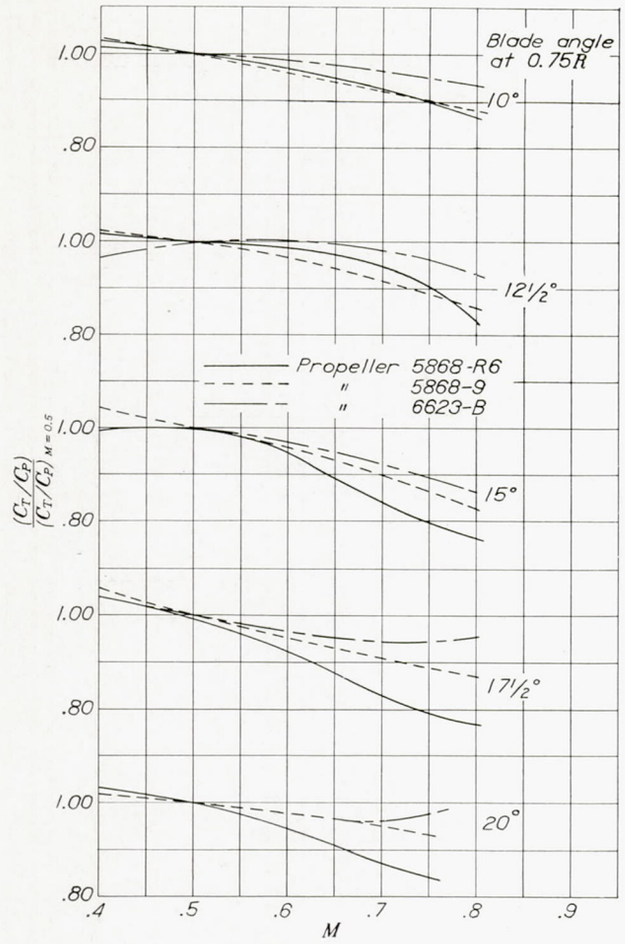


FIGURE 18.—Variation of propeller coefficients with tip-speed ratio for the 2-blade propellers.

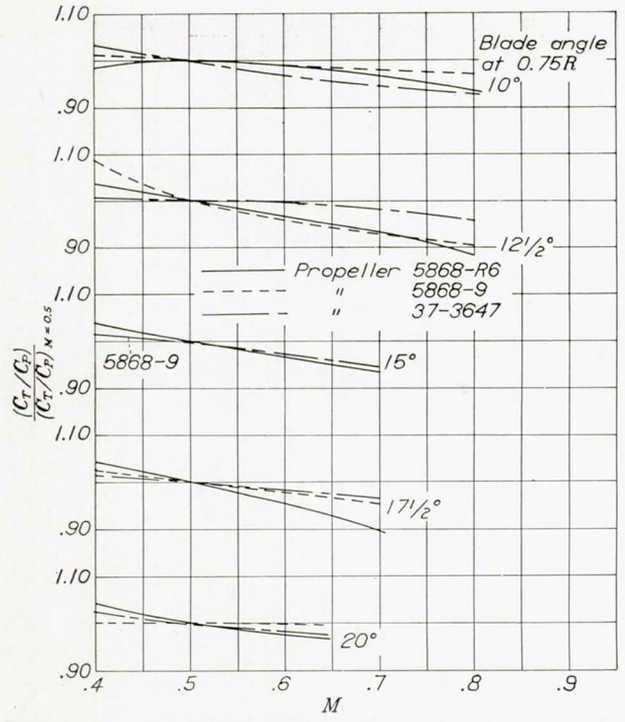


FIGURE 19.—Variation of propeller coefficients with tip-speed ratio for the 3-blade propellers and the 2-blade propeller 37-3647 having the same solidity.

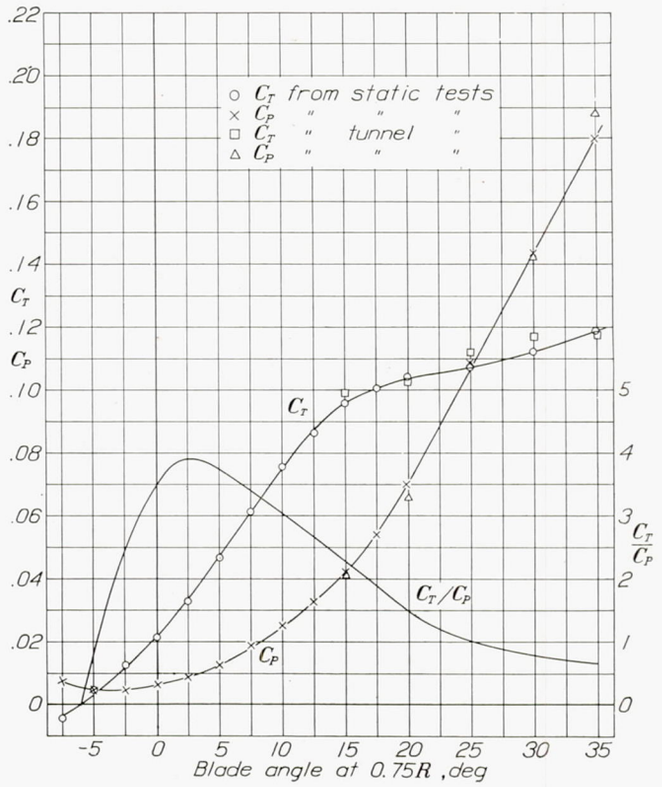


FIGURE 20.—Characteristics of 2-blade propeller 5868-9 at zero V/nD. M, 0.5.

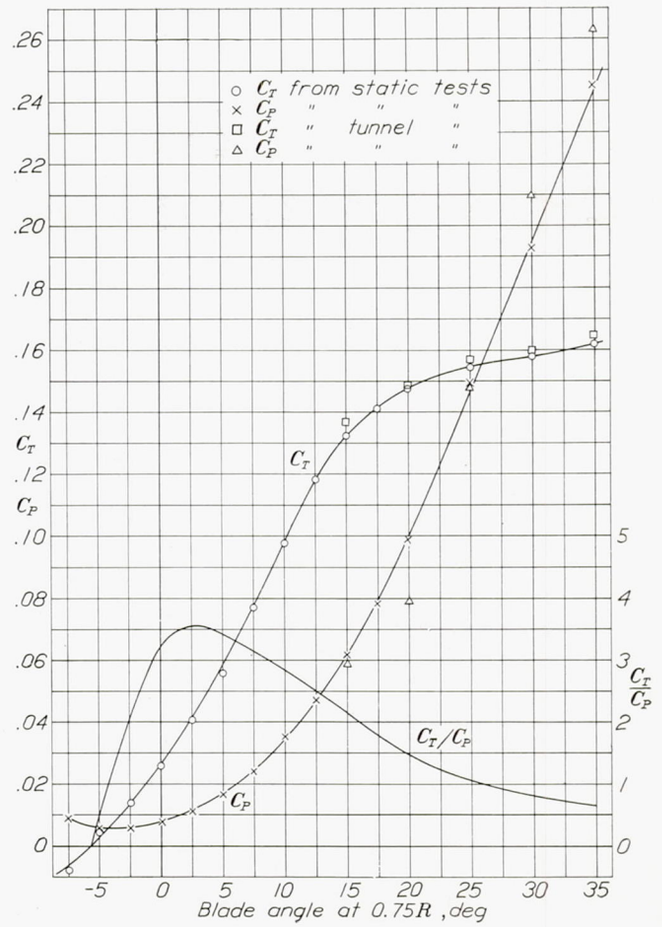


FIGURE 21.—Characteristics of 3-blade propeller 5868-9 at zero V/nD. M, 0.5.

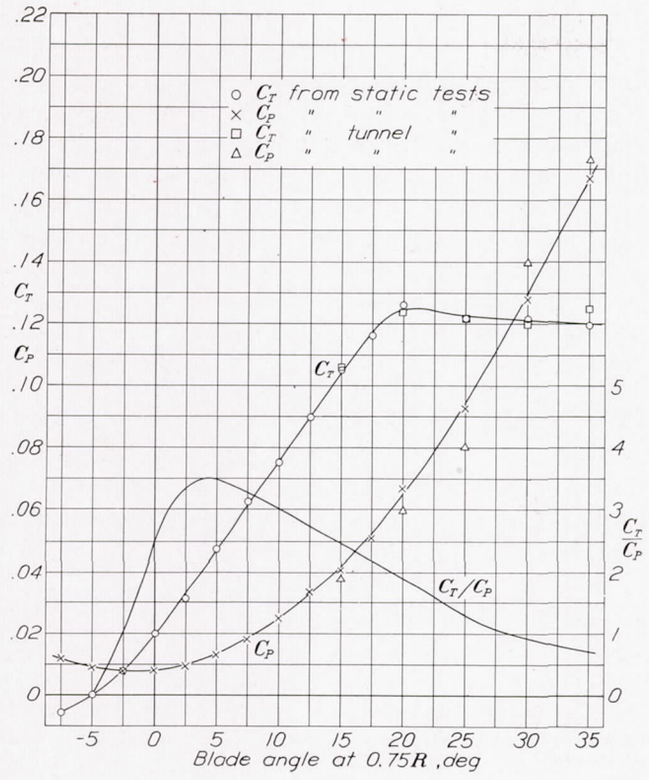


FIGURE 22.—Characteristics of 2-blade propeller 5868–R6 at zero V/nD. M, 0.5.

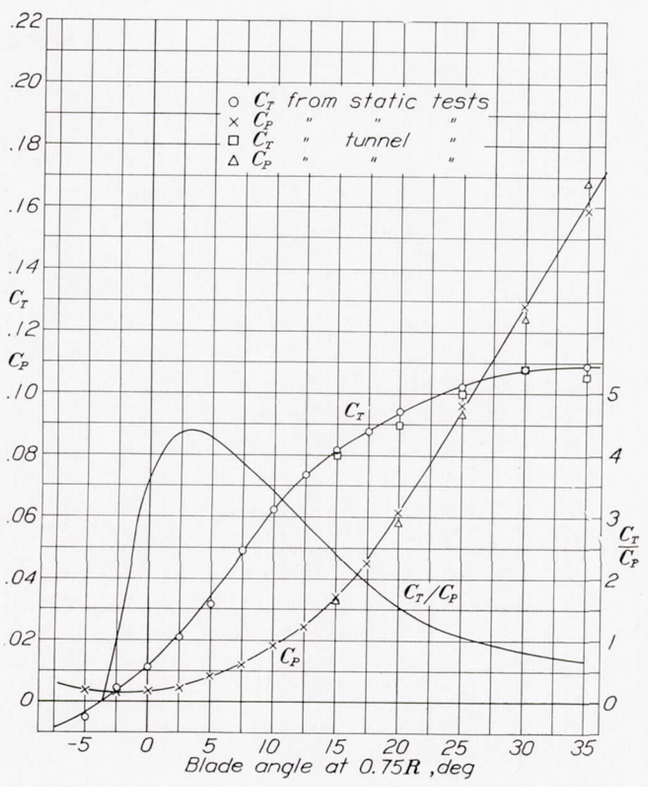


FIGURE 24.—Characteristics of 2-blade propeller 6623–B at zero V/nD. M, 0.5.

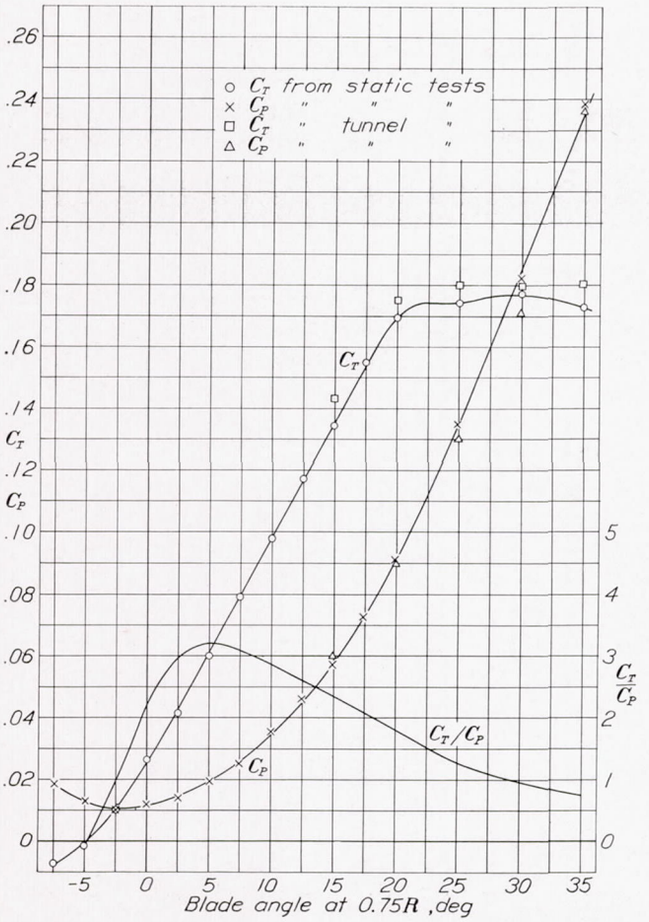


FIGURE 23.—Characteristics of 3-blade propeller 5868–R6 at zero V/nD. M, 0.5.

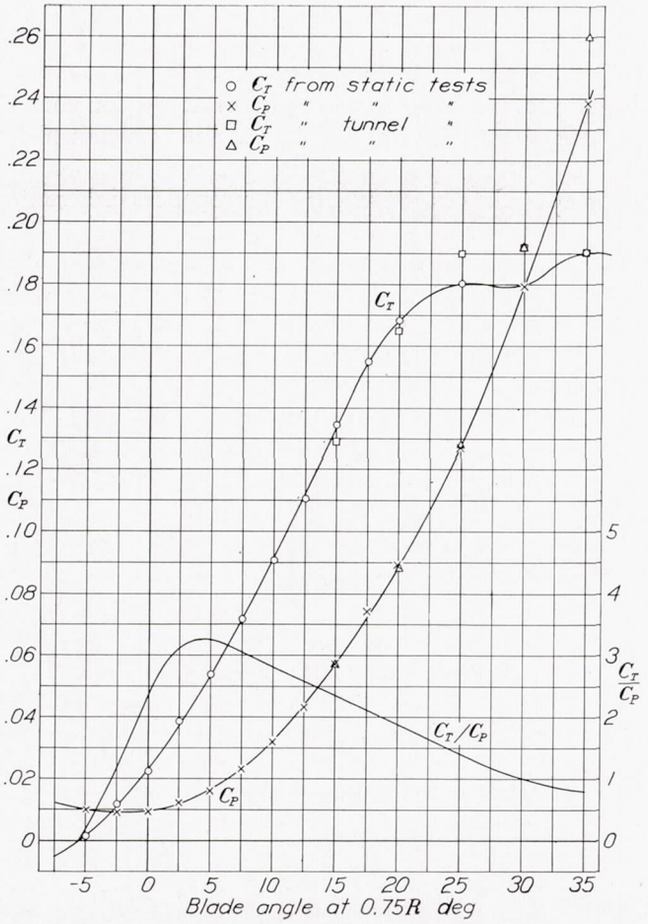


FIGURE 25.—Characteristics of 2-blade propeller 37–3647 at zero V/nD. M, 0.5.

WORKING CHARTS

Method of presentation.—Interesting and useful charts are produced by plotting static-thrust and static-power coefficients for a given tip speed against blade angle in a form similar to the one used in presenting airfoil coefficients. The coefficients are well adapted to this form of presentation and its familiarity adds to the understandability of the data. Figures 20 to 25 are plots of this kind for the six propellers operating at a tip speed of one-half the speed of sound ($M=0.5$). The ratio C_T/C_P, calculated from the faired curves, has also been plotted in the figures.

Comparison with airfoil curves.—The general shape of curves in figures 20 to 25 is very similar to that of the ordinary airfoil curves of C_L and C_D against angle of attack. One noticeable difference is that the C_T curve, corresponding to the C_L curve in airfoil-coefficient plots, is not straight through the unstalled range of blade angles; its slope decreases as zero C_T is approached. Probably the most important reason for a nonlinear variation of C_T with blade angle is that the pitch distribution changes with blade angle, as may be observed in figure 3. A similar and probably related phenomenon exists in wind-tunnel tests of propellers where the angle of attack of the blade at the $0.75R$ station (or any station), as calculated from the value of V/nD for zero thrust, decreases with blade-angle setting.

The curves in figures 20 to 25 indicate that the stall of the propeller is somewhat less severe than the stall of a conventional airfoil. This peculiarity is, of course, primarily due to the fact that the entire propeller blade does not stall at the same angle and also to the fact that the airfoil sections used in the propellers inherently have mild stalling characteristics.

Comparison with wind-tunnel data.—Each of the present propellers had been tested on the same engine and nacelle in the 20-foot wind tunnel. For comparison, the values of static thrust and static power obtained by extrapolating the wind-tunnel tests to $V/nD=0$ have been plotted in figures 20 to 25. The extrapolated wind-tunnel-test points are, in general, less regular than the static-test points; however, the tip speeds for the wind-tunnel tests varied slightly.

Use of working charts.—Figures 18 and 19, as well as figures 20 to 25, are considered to be working charts; from these figures the static thrust and the static power for any of the propellers tested may be obtained. For fixed-pitch propellers, the values of C_T, C_P, and C_T/C_P may be picked off at the design blade angle. These values are for a tip speed of one-half the speed of sound and may be corrected to the design tip speed by applying a factor obtained from figures 18 and 19. The value of C_T/C_P corrected for tip speed may be converted to the following useful coefficient form:

$$\frac{C_T}{C_P}=\frac{T_e\rho n^3D^5}{P\rho n^2D^4}=\frac{T_enD}{P}=\frac{T_enD}{2\pi nQ}=\frac{T_eD}{2\pi Q}$$

where Q is the engine torque. Most engines likely to be used with fixed-pitch propellers will have approximately constant torque (full-power torque) through the take-off and the flying ranges; thus, with the calculated value of engine torque and the design diameter, the effective static thrust can be readily calculated.

For controllable constant-speed propellers, where power coefficient, power, and engine speed remain constant during the take-off, the value of C_T/C_P for $V/nD=0$ may be immediately obtained from figures 20 to 25 and corrected to design tip speed as before. The effective static thrust is then calculated from the previously given relation $\frac{C_T}{C_P}=\frac{T_enD}{P}$, where all the terms except T_e are known.

As the data given herein were obtained with a nacelle alone, an increment of thrust should be deducted from the computed values to account for the drag of the parts of the airplane, other than the nacelle, that lie in the slipstream. This factor is, however, partly compensated for by the fact that there were five struts and several wires in the test set-up, the drag of which, like that of the nacelle, registered on the thrust balance as part of the total effective thrust.

COMPARISONS

As the speed of an airplane increases from zero at the beginning of the take-off run to its maximum value, the angles of attack of the propeller blade sections are continuously decreasing. The airfoil section at $0.75R$, for example, will have an angle of attack that decreases from, say, 20° at the beginning of the take-off run to about 0° at high speed. It appears, therefore, that the performance of a propeller through its flight range may be represented, qualitatively at least, by its static performance through the range of blade angles from about −5° to 25° at $0.75R$. A comparison of the static coefficients, through this blade-angle range, of two propellers of equal solidity will give a fairly good qualitative indication of their relative flight performances. The following comparisons, which are shown in figures 26 to 29, were made with these ideas in mind.

Propellers with 2 and 3 blades.—The static-coefficient curves for the 2-blade and the 3-blade propellers 5868–9 are shown in figure 26. As might be expected, the 2-blade propeller has a higher value of C_T/C_P in the unstalled range although, in the stalled range, the 3-blade propeller is slightly better. The greater inflow velocity of the 3-blade propeller largely accounts for both of these phenomena. The thrust coefficient C_{T_3} of the 3-blade propeller in the unstalled range is not 50 percent greater than the thrust coefficient C_{T_2} of the 2-blade propeller; for example, the ratio C_{T_3}/C_{T_2} at a blade angle of 10° has a value of 1.32 rather than the value 1.5 that might possibly be expected. This difference is also due to the greater inflow velocity of the 3-blade propeller.

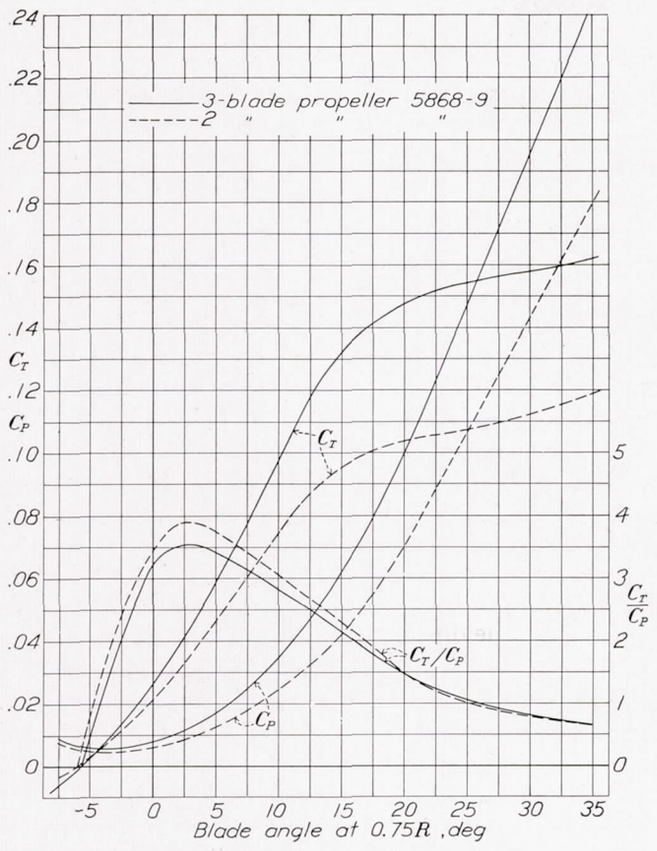


FIGURE 26.—Comparison of static aerodynamic characteristics of 2-blade and 3-blade propellers. M, 0.5.

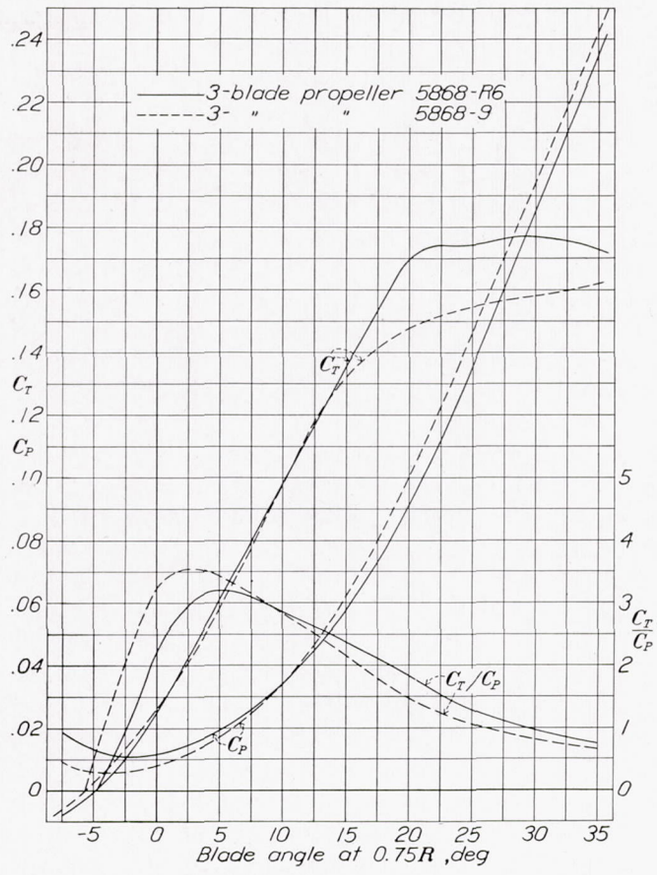
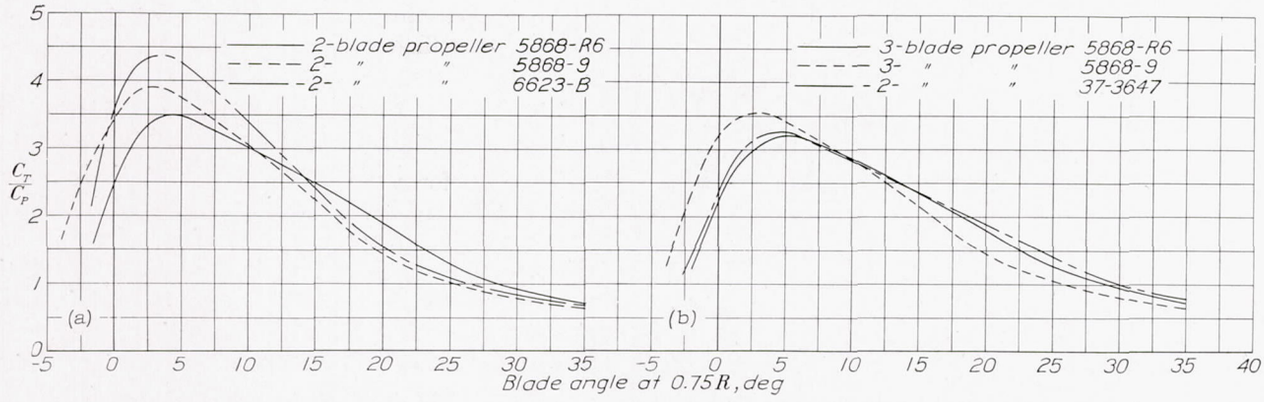
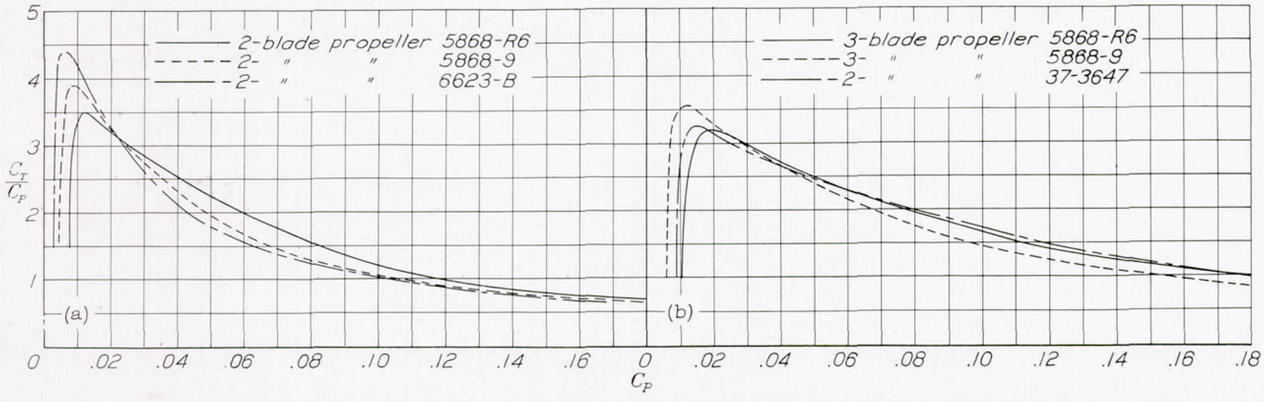


FIGURE 27.—Comparison of static aerodynamic characteristics of 3-blade propellers having Clark Y (5868–9) and R. A. F. 6 (5868–R6) airfoil sections. M, 0.5.



(a) 2-blade propellers having the same solidity. (b) 3-blade propellers and 2-blade propeller having the same solidity.

FIGURE 28.—Comparison of propeller characteristics. C_T/C_P against blade angle; V/nD, 0; M, 0.5.



(a) 2-blade propellers having the same solidity. (b) 3-blade propellers and 2-blade propeller having the same solidity.

FIGURE 29.—Comparison of propeller characteristics. C_T/C_P against C_P; V/nD, 0; M, 0.5.

It should be pointed out that the comparison shown in figure 26 is not of a practical nature because the two propellers compared have different power-absorption characteristics.

Propellers with Clark Y and R. A. F. 6 airfoil sections.—Figure 27 shows the static coefficients for the 3-blade propellers with Clark Y and R. A. F. 6 airfoil sections (propellers 5868–9 and 5868–R6). These curves substantiate a fact that has long been known; namely, at low tip speeds, the R. A. F. 6 section is better than the Clark Y section at high angles of attack but, owing to higher profile drag, is poorer at low angles of attack. From these curves of static coefficients, it can be readily predicted that a propeller with an R. A. F. 6 section will have a lower peak efficiency than one with a Clark Y section; and, in the take-off range, tip-speed effects being neglected, a propeller with an R. A. F. 6 section will have a higher efficiency than a propeller with a Clark Y section, provided that the propellers are identical in all respects except section.

It should be mentioned that the higher take-off efficiency of the propeller with an R. A. F. 6 section applies mainly to fixed-pitch propellers operating at low tip speeds. When the performances of controllable propellers having Clark Y and R. A. F. 6 airfoil sections are compared on the basis of constant C_P, it will be noted (see fig. 27) that, owing to its higher power absorption at high blade angles, the blades of the propeller with a Clark Y section will operate at a lower blade angle than those of the propeller with an R. A. F. 6 section; and, since C_T/C_P rapidly increases with a decrease in blade angle, the difference between the values of the C_T/C_P ratios for the two propellers may be much reduced. The serious effects of compressibility on the performance of the R. A. F. 6 section, as indicated in figures 18 and 19, also work to the disadvantage of the propeller of R. A. F. 6 section in the take-off range. When all factors are taken into consideration, a controllable propeller of R. A. F. 6 section will have very little, if any, advantage over a controllable propeller of Clark Y section in the take-off range.

Propellers having the same solidity.—The ratio C_T/C_P for groups of propellers having the same solidity (ratio of blade area to disk area) is plotted against blade angle in figure 28 and against power coefficient in figure 29.

The values of C_T/C_P were plotted against both blade angle and C_P for convenience in comparing fixed-pitch and controllable-pitch propellers; in such cases, blade angle and C_P are, respectively, fundamental design factors.

Little discussion of the figures is necessary except to note that, in general, the propellers which are best in the range of blade angles and C_P representing take-off are poorest in the range representing high-speed flight. Apparently, a compromise must be struck between high-speed and take-off performance although, for reasons given earlier, the high-speed condition should probably be given the greater consideration.

CONVERSION OF PROPELLER COEFFICIENTS INTO AIRFOIL CHARACTERISTICS

One purpose of this report, as mentioned in the introduction, was to examine the single-point method of obtaining airfoil characteristics (C_L, C_D, and α) from propeller data with especial regard to its use with the present static propeller data. It was also the purpose of this report to determine with what degree of accuracy wind-tunnel-test data on propellers might be replaced by static propeller data, more easily and cheaply obtained, that had been converted to "wind-tunnel data" (data for range of V/nD values) by the single-point method. The method has been applied in a few cases to N. A. C. A. wind-tunnel data for propellers and to the present static propeller data.

Description of method.—The single-point method as described in references 4 and 5 is founded on the simplifying assumption that the differential thrust and torque coefficients, $dC_T/d(x^2)$ and $dC_Q/d(x^2)$, when plotted against x^2 produce curves which are semiellipses. Granting this assumption, the total thrust and the total torque coefficients are merely the product of $\pi/4$ and the value of the differential coefficients at $x^2=0.5$. The station representing the whole propeller is thus found at $x^2=(r/R)^2=0.5$, or $x=r/R=0.707$ and is, for convenience, taken as the station at $0.70R$. Conversely, the differential thrust and torque coefficients for the $0.70R$ station may be easily obtained if the total thrust and torque coefficients are known from propeller tests.

With values of C_T, C_P, V/nD, and blade angle, obtained from wind-tunnel tests, the differential thrust and torque coefficients for the $0.70R$ station are easily obtained and are then, by simple geometric relations, converted to lift and drag coefficients for the $0.70R$ station. If, for any one blade angle, the calculations are repeated for values of C_T and C_P obtained at a series of values of V/nD in the operating range, a polar curve of C_L against C_D for the $0.70R$ station, which is assumed to represent the whole propeller, may be plotted. The process is slightly different where static data are used since, in that case, $V/nD=0$. The polar curve may be obtained, however, by using the values of C_T and C_P at a series of blade angles from about $-5°$ to $35°$ at $0.75R$.

The development of the method is carried further by introducing factors representing the induced velocity and Goldstein's correction factor for a finite number of blades. In this manner, C_D is broken down into its components, C_{D_i} and C_{D_0}; the angle of attack of the section, α_∞, is also obtained. The coefficients C_L and C_{D_0} reveal certain fundamental characteristics of the propeller and may be used as a basis of comparison.

It is implied in references 4 and 5 that the polars of C_L against C_{D_0} should be the same for static or wind-tunnel data and for all solidities and blade angles.

Airfoil polar curves from propeller data.—Figures 30 and 31 show the polars for the 2- and the 3-blade propellers 5868–9 calculated by the single-point method. The calculations were made from the present static-thrust data and also from the wind-tunnel-test data of the same propellers and nacelle given in reference 8. It is observed that the polars from wind-tunnel tests at the three different blade angles are not identical, as the theory indicates they should be. The polars for the 15° and the 25° blade angles are probably as close as could be expected but the polar for the 35° blade angle is separated from the others by a fairly large amount. Further, the polars obtained from the static tests do not coincide with any of the polars from the wind-tunnel tests.

Possible causes of discrepancies in polars.—Although the single-point method is based on the assumption that the curves of differential thrust and power coefficients are ellipses when plotted against x^2, the method appears to apply reasonably well to cases where the curves vary considerably from ellipses. Generally, in such cases, the value of the differential thrust and power coefficients for the single representative station ($0.70R$) is approximately, but not exactly, equal to the total thrust and power coefficients divided by $\pi/4$.

There are several reasons why these polars do not confirm the theory, that is, why the curves are not all identical, and most of the reasons point to factors that render the assumptions of the single-point method not wholly justifiable. Two of the reasons that apply to both static-test and wind-tunnel-test polars may be stated as follows:

1. The theory strictly applies only to propellers without bodies. The use of effective thrust rather than actual propeller thrust and, in addition, the interference of the body may tend to make the single-point assumption unreliable.

2. The propeller from which Driggs (reference 5) obtained the test data to justify the single-point assumption, as well as the propellers for which the method has proved so successful in Great Britain, differs in blade-shank shape from the propellers of the present tests. The present propellers have long, cylindrical, drag-producing shanks (fig. 3); whereas, the other propellers mentioned have relatively thin airfoil sections extending nearly to the hubs. This difference in blade shape will have some effect on the thrust- and the torque-distribution curves.

Another reason why static-test polars should not coincide with the wind-tunnel-test polars and also why the polars calculated from wind-tunnel tests at different blade angles do not agree is that the blade angle and

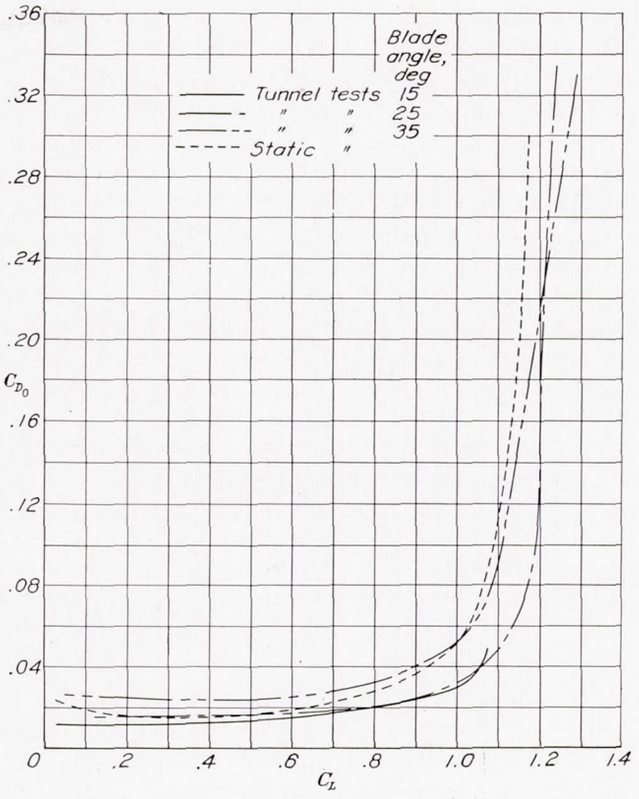


FIGURE 30.—Comparison of polars obtained from wind-tunnel tests and from static tests of 2-blade propeller 5868–9.

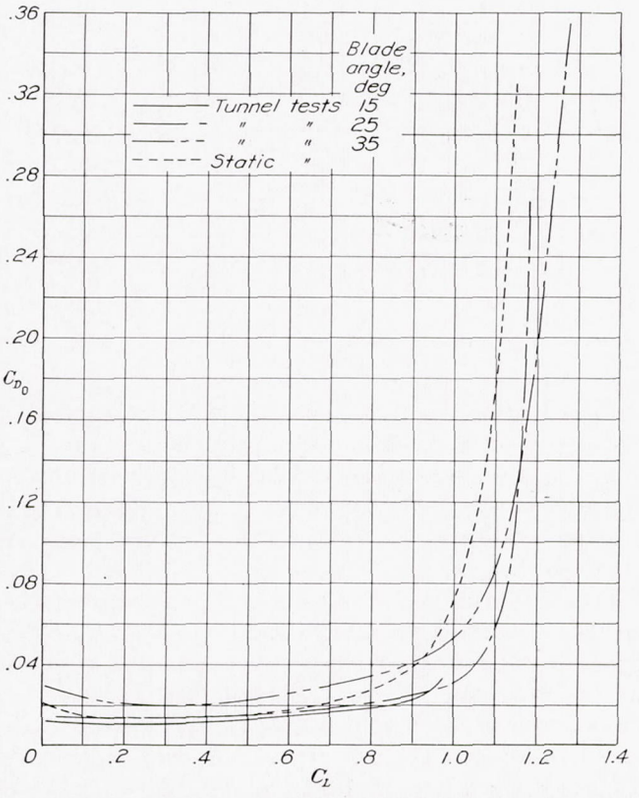


FIGURE 31.—Comparison of polars obtained from wind-tunnel tests and from static tests of 3-blade propeller 5868–9.

therefore the pitch distribution (see fig. 3) are continuously varying from point to point in the static polar; whereas, in any particular wind-tunnel-test polar, the blade angle and the pitch distribution remain constant. The varying pitch distribution probably accounts for some of the curvature in the static-test C_L curve shown in figure 32.

The difference between the airfoil coefficients obtained from static and from wind-tunnel tests may also be due to the fact that the flow around the propeller in the static condition differs considerably from the flow that exists when the propeller is moving or is in a wind-tunnel air stream. In the static condition, the propeller

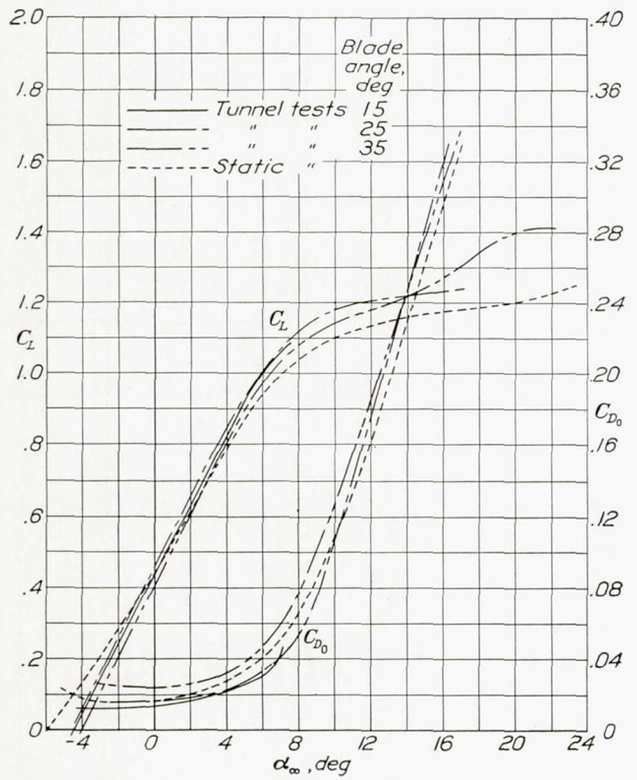


FIGURE 32.—Comparison of lift and drag coefficients obtained from wind-tunnel and static tests for 2-blade propeller 5868-9.

tips are working in a strong vortex that tends to reduce the effective aspect ratio of the propeller and also, perhaps, its maximum thrust. This fact may account for the lesser slope of the static lift curve in figure 32 and also for the lower maximum values of the static lift coefficients in figures 30 to 32.

Propeller polars for nacelle with spinners.—When all the reasons why the single-point method should not apply to tests of these types are considered, it is surprising how well the method does work. From the preceding discussion, it appears that the method should apply with better accuracy to tests where a spinner was used to cover up the hub and at least part of the cylindrical blade shanks. Results from wind-tunnel tests of the present propellers and nacelle with a spinner were available from reference 6. Figure 33 shows the points of the polars calculated from wind-tunnel-test data on the arrangement designated spinner 1 in reference 6. A mean line has been drawn through the points for the three blade angles. Inasmuch as no static tests with a spinner were made, the static and the wind-tunnel-test polars, with spinner, cannot be compared. The static polars from figures 30 and 31 (without spinner) are shown again in figure 33 for comparison. Theoretically, the two static polars should coincide.

Figure 33 indicates that the single-point method of propeller analysis can be used fairly successfully for wind-tunnel tests of modern propellers provided that the hub and the cylindrical blade shanks are covered by a spinner. The propeller shanks should have a smaller effect on a radial engine where they are shielded by the engine. Where only data "without spinner" are available for a propeller operating in front of a liquid-cooled-engine nacelle, as in the present tests, the effect of a spinner may be obtained by adding an increment of thrust to account for the drag of the hub and the shanks. Neglecting the effect of inflow velocity, which for this purpose should be permissible, the increment of thrust will vary with V/nD in the following manner: $\Delta C_T = k(V/nD)^2$, where k is a constant the magnitude of which depends upon the propeller and the nacelle. The value of k for the propellers and the nacelle of the present tests is about 0.0007 for 2-blade propellers and about 0.00105 for 3-blade propellers. It is clear from the preceding relation that, for static tests, $\Delta C_T = 0$ and so, in figure 33, the wind-tunnel-test polars "with spinner" and the static-test polars "without spinner" are comparable.

Proper use for single-point method applied to static-test data.—The case for the static-test polars appears, from figure 33, still to be unfavorable although the degree of accuracy may be sufficient for some purposes. The wind-tunnel-test polars for the 2- and the 3-blade propellers more nearly coincide than do the static-test polars for the 2- and the 3-blade propellers. This situation indicates that Goldstein's correction factor for a finite number of blades may not apply so well to static tests as it does to wind-tunnel tests.

The present data seem to indicate that airfoil coefficients obtained by the single-point method from static tests cannot be converted into wind-tunnel propeller coefficients with any high degree of accuracy. It appears that the field of usefulness of the static-test polar is rather in making qualitative comparisons between propellers of not too dissimilar design. For this purpose, simple static tests may replace the more complicated and more expensive wind-tunnel tests. It is admitted that the evidence upon which the conclusions in this section are based is insufficient to be entirely conclusive.

Comparisons of static-test polars.—Static-test polars can undoubtedly be used in comparing propellers iden-

tical in every respect except airfoil section. Such a comparison has been made in figure 34. This figure confirms the information given in figure 28 that the sections which are best at high angles of attack (take-off range) are poorest at low angles of attack (peak efficiency, high-speed range). The propeller with the Clark Y section appears to be a good compromise.

A comparison of the static-test polars for the 3-blade propeller 5868–R6 and the 2-blade propeller 37–3647, having the same solidity, is given in figure 35. Apparently, there is little to choose between the two although, when the polars are converted to "wind-tunnel" propeller data, the Goldstein factor will favor the 3-blade propeller and the 3-blade propeller may then, as indicated in reference 8, have a higher peak efficiency than the 2-blade propeller.

The single-point method of obtaining airfoil characteristics from static tests may be useful in studying the effects of compressibility. An indication of the use of the method in this connection is given in figure 17 which, as previously explained, shows the variation with tip speed of C_L, C_D, C_{D_i}, and C_{D_0} for one blade angle.

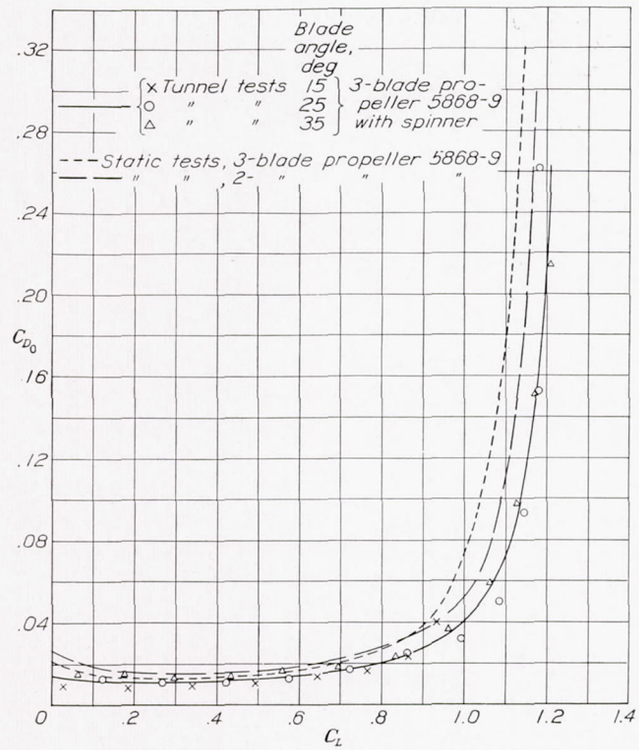


FIGURE 33.—Comparison of polars obtained from wind-tunnel and static tests of propeller 5868–9.

CONCLUSIONS

1. The static-thrust and the static-power coefficients for the propellers of the present tests varied consider-

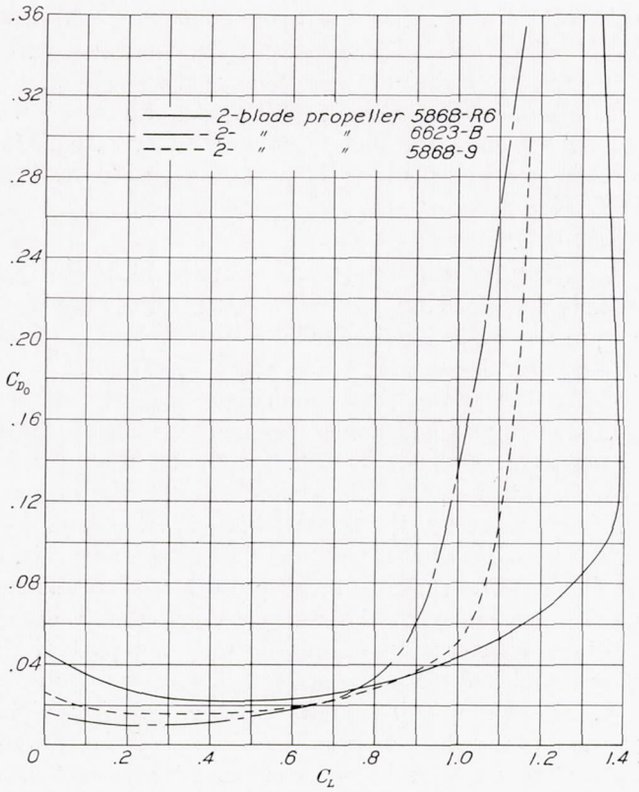


FIGURE 34.—Comparison of polars obtained from static tests of three 2-blade propellers having different airfoil sections. M, 0.5.

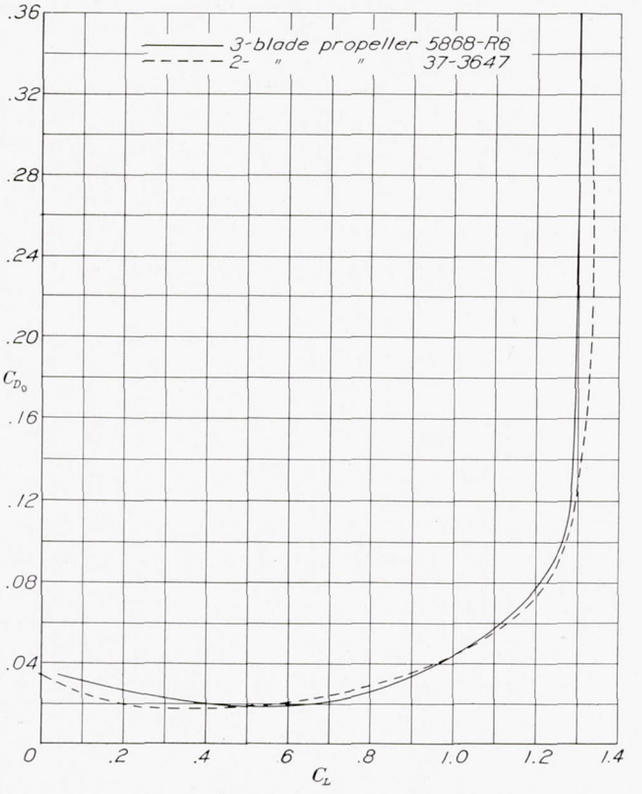


FIGURE 35.—Comparison of polars obtained from static tests of 2- and 3-blade propellers having the same solidity. M, 0.5.

ably with tip speed in the blade-angle range from 5° to 17½° at $0.75R$. Above the stall, no consistent variation of these coefficients with tip speed was noted.

2. Decrease of the ratio C_T/C_P with tip speed was most marked for propellers having R. A. F. 6 airfoil sections, least marked for the propeller with N. A. C. A. 2400–34 series sections, and more marked for 2-blade than for 3-blade propellers.

3. Although the effect of compressibility on the 2-blade propeller 5868–R6 was very marked, the effect on another propeller similar in every respect except for a 50-percent increase in blade width was small.

4. The propellers that reached the highest values of C_T/C_P at high blade angles reached the lowest values at low blade angles. This fact indicates that, for the propellers tested, the ones which have the highest peak efficiency will have the poorest take-off efficiency.

5. The single-point method of calculating airfoil coefficients from wind-tunnel propeller data was not particularly successful for the present propellers except where a spinner covered up the hub and part of the long cylindrical blade shanks.

6. The single-point method of calculating airfoil characteristics did not give the same coefficients when applied to both static-test and wind-tunnel-test data.

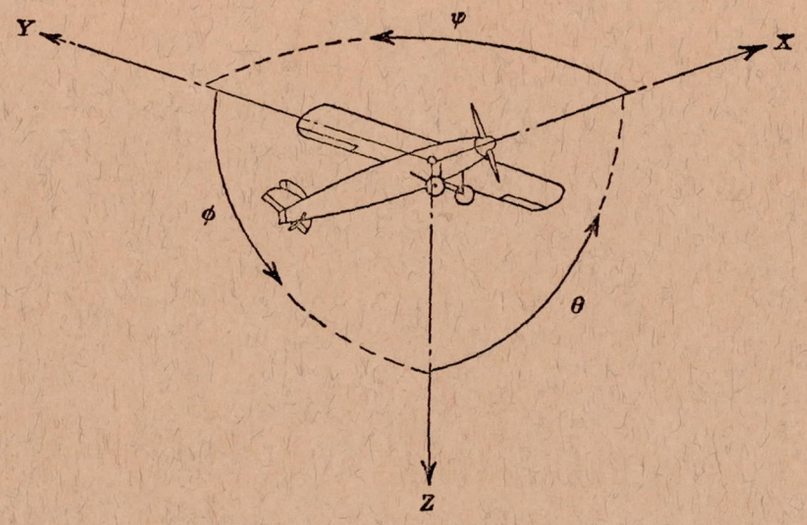
7. Whereas the single-point method should be of much value for comparing propellers, it does not appear likely that this method will displace wind-tunnel research for establishing the absolute values of propeller coefficients.

LANGLEY MEMORIAL AERONAUTICAL LABORATORY,
NATIONAL ADVISORY COMMITTEE FOR AERONAUTICS,
LANGLEY FIELD, VA., *January 25, 1939.*

REFERENCES

1. Diehl, Walter S.: The Calculation of Take-Off Run. T. R. No. 450, N. A. C. A., 1932.
2. Diehl, Walter S.: Static Thrust of Airplane Propellers. T. R. No. 447, N. A. C. A., 1932.
3. Enos, Louis H.: Some Full Scale Static Propeller Characteristics. Jour. Aero. Sci., vol. 5, no. 1, Nov. 1937, pp. 25–28.
4. Lock, C. N. H.: A Graphical Method of Calculating the Performance of an Airscrew. R. & M. No. 1675, British A. R. C., 1935.
5. Driggs, Ivan H.: Simplified Propeller Calculations. Jour. Aero. Sci., vol. 5, no. 9, July 1938, pp. 337–344.
6. Biermann, David, and Hartman, Edwin P.: Tests of Five Full-Scale Propellers in the Presence of a Radial and a Liquid-Cooled Engine Nacelle, Including Tests of Two Spinners. T. R. No. 642, N. A. C. A., 1938.
7. Biermann, David, and Hartman, Edwin P.: The Effect of Compressibility on Eight Full-Scale Propellers Operating in the Take-Off and Climbing Range. T. R. No. 639, N. A. C. A., 1938.
8. Hartman, Edwin P., and Biermann, David: The Aerodynamic Characteristics of Full-Scale Propellers Having 2, 3, and 4 Blades of Clark Y and R. A. F. 6 Airfoil Sections. T. R. No. 640, N. A. C. A., 1938.

U. S. GOVERNMENT PRINTING OFFICE: 1940



Positive directions of axes and angles (forces and moments) are shown by arrows

Axis		Force (parallel to axis) symbol	Moment about axis			Angle		Velocities	
Designation	Symbol		Designation	Symbol	Positive direction	Designation	Symbol	Linear (component along axis)	Angular
Longitudinal	X	X	Rolling	L	$Y \longrightarrow Z$	Roll	ϕ	u	p
Lateral	Y	Y	Pitching	M	$Z \longrightarrow X$	Pitch	θ	v	q
Normal	Z	Z	Yawing	N	$X \longrightarrow Y$	Yaw	ψ	w	r

Absolute coefficients of moment

$C_l = \frac{L}{qbS}$ (rolling) $\quad C_m = \frac{M}{qcS}$ (pitching) $\quad C_n = \frac{N}{qbS}$ (yawing)

Angle of set of control surface (relative to neutral position), δ. (Indicate surface by proper subscript.)

4. PROPELLER SYMBOLS

D, Diameter

p, Geometric pitch

p/D, Pitch ratio

V', Inflow velocity

V_s, Slipstream velocity

T, Thrust, absolute coefficient $C_T = \frac{T}{\rho n^2 D^4}$

Q, Torque, absolute coefficient $C_Q = \frac{Q}{\rho n^2 D^5}$

P, Power, absolute coefficient $C_P = \frac{P}{\rho n^3 D^5}$

C_s, Speed-power coefficient $= \sqrt[5]{\frac{\rho V^5}{P n^2}}$

η, Efficiency

n, Revolutions per second, r.p.s.

Φ, Effective helix angle $= \tan^{-1}\left(\frac{V}{2\pi r n}\right)$

5. NUMERICAL RELATIONS

1 hp.=76.04 kg-m/s=550 ft-lb./sec.
1 metric horsepower=1.0132 hp.
1 m.p.h.=0.4470 m.p.s.
1 m.p.s.=2.2369 m.p.h.

1 lb.=0.4536 kg.
1 kg=2.2046 lb.
1 mi.=1,609.35 m=5,280 ft.
1 m=3.2808 ft.